

Functional networks from inverse modeling of neural population activity

Simona Cocco^a, Rémi Monasson^b, Lorenzo Posani^{a,b} and Gaia Tavoni^c

Abstract

The availability of large-scale neural multi-electrode or optical recordings make now possible the modelling of the simultaneous activities of tens to thousand of neurons. One promising approach relies on the inference of detailed functional connectivity between the recorded cells, that is, of an effective coupling network reproducing the correlation structure of the spiking events. Here we report some recent applications of those approaches to retinal, hippocampal, and cortical data, illustrating in particular how functional coupling networks may be useful to decode complex brain representations, and how their changes may be tracked in behaving animals, with a possible connection to behavioral learning. Statistical, theoretical, and neurobiological issues raised by the inverse modeling of population activity are discussed.

Addresses

^a Laboratoire de Physique Statistique, Ecole Normale Supérieure, PSL Research and CNRS – UMR 8550, Paris Sorbonne UPMC, 24 rue Lhomond, 75005 Paris, France

^b Laboratoire de Physique Théorique, Ecole Normale Supérieure, PSL Research and CNRS – UMR 8549, Paris Sorbonne UPMC, 24 rue Lhomond, 75005 Paris, France

^c Department of Physics and Astronomy, University of Pennsylvania, Philadelphia, USA

Corresponding author: Cocco, Simona

Current Opinion in Systems Biology 2017, 3:103–110

This review comes from a themed issue on **Mathematical modelling, Dynamics of brain activity at the systems level (2017)**

Edited by **Marcelo O. Magnasco**

For a complete overview see the [Issue](#) and the [Editorial](#)

Available online 4 May 2017

<http://dx.doi.org/10.1016/j.coisb.2017.04.017>

2452-3100/© 2017 Elsevier Ltd. All rights reserved.

Keywords

Functional connectivity, Inference, Ising model, Cell assemblies, Memory replay, Map decoding, Retina, Prefrontal cortex, Hippocampus.

Introduction

Functional connectivity across neurons has long been investigated through pairwise correlations [1,2], independently of the activity of the other recorded neurons. The availability of large population neural recordings, with tens to thousands of cells [3–9], has recently

fostered interest for inverse approaches to reconstruct functional connectivity [10,11], in particular from snapshots of the activity [12,13] (Box 1). These approaches are coherent in that they process all recorded cells together, and are able to disentangle direct correlations between cells from indirect effects mediated through other recorded neurons [11,14]. We report below some applications to various brain areas, in connection with the following issues:

1. Functional couplings a priori vary with the sampling conditions (Box 2), such as brain state or external stimuli (Box 2). How strong is this variation, and what features remain invariant across different states?
2. Are functional models accurate enough to identify (decode) brain states [15–17], even in the absence of any sensory correlate?
3. Can we measure experience-related changes in functional couplings [18,19], and do they reflect properties expected for physiological plasticity [20,21]?
4. Are functional networks helpful to identify cell assemblies, postulated by Hebb to be the central units of neural computation and memories [22,7,23,18,24]?

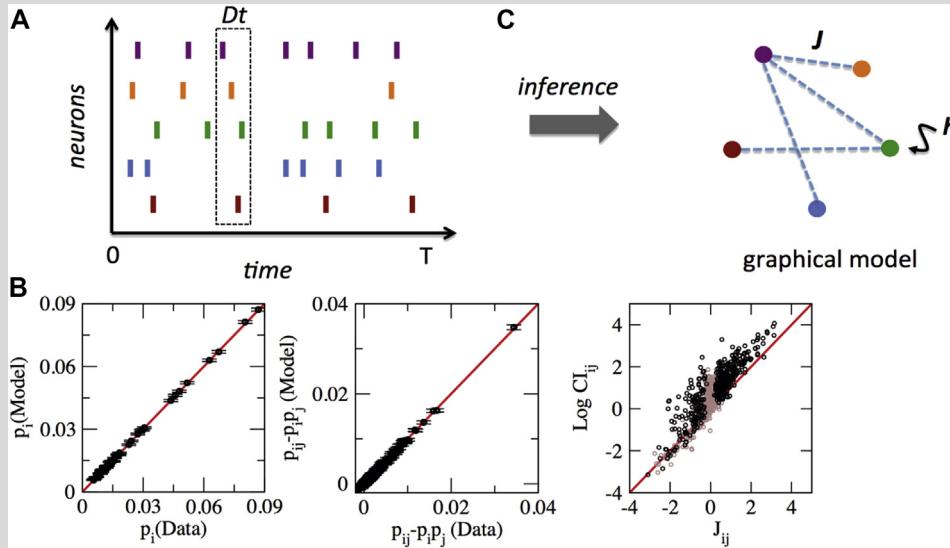
Functional networks show both invariant structure and specificity with respect to neural states

Functional connectivity reproduces the patterns of correlations in the neural activity across the recorded population. Those correlations reflect both the synaptic underlying interactions, as well as common inputs specific to the environmental, sensorial or cognitive state. To study the importance of both contributions we focus on three multi-electrode recording data sets (DS), in which the same cells were recorded with different external stimuli or conditions:

(DS1) salamander Retina ganglion cell (RGC) were recorded in the absence of light (dark) and with a randomly flickering checkerboard stimulus (flicker) [4]. Figure 1a shows the effective couplings between RGC, located at the centers of their receptive fields in the retinal plane [14]. In both dark and flickers stimuli a short-range network of large and positive couplings is found, similarly to [13], presumably due to gap junctions

Box 1. Functional connectivity models for neural data

Data consists of the times of all spikes emitted by a population of N neurons during a recording of duration T (**A**). We first discretize the data into time bins $t = 1, \dots, T/Dt$ of width Dt , and define for each bin a variable $s_{i,t} = 1$ if neuron i has emitted one or more spikes, and 0 otherwise. Typical Dt values range from 10 to 100 ms depending on the recorded brain area.



Inference of functional model. **A.** Multi-electrode or optical recordings are analyzed to obtain the raster plot of the neural activity (left). Activities are binned into time windows of duration Dt (dashed box) to define the configuration $S_t = (s_{1t}, s_{2t}, \dots, s_{Nt})$. The functional network J_{ij} describing the spiking dependencies among the neuron activities is then inferred, together with the local inputs h_i acting on the neurons. **B.** Single-cell firing probabilities p_i and pairwise correlations $p_{ij} - p_i p_j$ in data (x-axis) vs. predictions from inferred Ising model (y-axis). **C.** Scatterplot of inferred couplings J_{ij} vs. \log correlation indices $C_{ij} = p_{ij}/p_i p_j$ [42]. Data in **B** and **C** are RGC recordings from Ref. [12].

We look for a distribution model over the set of activity configurations in time bins, $S_t = (s_{1t}, s_{2t}, \dots, s_{Nt})$. In the simplest model, neural cells are supposed to spike independently of each other. This model is generally poor, as it cannot reproduce correlations between spiking events [12]. In functional-connectivity models the probability that neuron i is active ($s_i = 1$) is conditioned to the activities s_j of the other neurons j :

$$P_{cond}(s_i = 1 | \{s_j, j \neq i\}) = \Phi \left(\sum_{j \neq i} J_{ij} s_j + h_i \right) \tag{1}$$

where $\Phi(x)$ is a sigmoidal increasing function of its argument x . The local input h_i controls the average activity of neuron i (the higher the input, the larger the activity), while the couplings J_{ij} encode the conditional dependence of the activities of neurons i and j (large positive, respectively, negative couplings correspond to pairs of neurons with correlated, respectively, anticorrelated activities). In practice the N inputs and $N(N - 1)/2$ couplings are fitted to maximize the probability of the data configurations; this is a non-trivial computational problem, which can be tackled with various approximate inference techniques [56–59]. A natural choice is $\Phi(x) = \frac{e^x}{1+e^x}$, which corresponds to the well-studied Ising model of statistical physics, and to a simple expression of the probability of activity configurations,

$$P(s_1, s_2, \dots, s_N) \propto \exp \left(\sum_{j < i} J_{ij} s_i s_j + \sum_i h_i s_i \right), \tag{2}$$

up to some multiplicative normalization factor.

When only $N = 2$ cells are recorded the unique coupling, J_{12} , is related to the correlation index, C_{12} , equal to the ratio of the probability that neurons 1 and 2 both spike in a time bin, over the product of their individual spiking probabilities, through $J_{12} = \log C_{12}$. When more cells are recorded no general relationship exists between couplings and correlation indices [42], unless the activity is extremely sparse [41].

We stress that Eqs. [1] & [2] are approximate; modified Ising models, including non linear combinations of the neural activities in the argument of Φ , have been proposed [53].

Box 2. Sampling issues

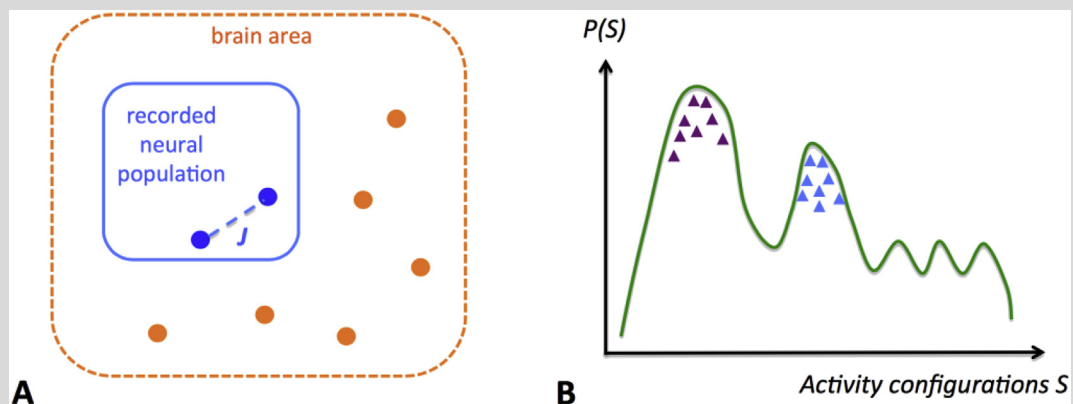
An important issue is whether couplings are accurately inferred. This question may be considered from different points of views.

How much data are needed? Errors on statistical observables, e.g. 1- and 2-neuron spiking probabilities, are of the order of $1/\sqrt{B}$, when the number $B = T/Dt$ of time bins is large. Since there are $\sim N^2$ pairs of neurons, we expect, from extreme value theory, the largest error to be $\sim \sqrt{\log N}/\sqrt{B}$. This value is the minimal coupling J (in absolute value) that can be inferred reliably from B configurations [58].

How to avoid overfitting data? Maximizing the probability of the data set with the Ising model can lead to overfitting, that is, to fine-tuning of couplings to reproduce details in the data due to partial sampling rather than to their underlying structure. An illustration is offered by the case of N independent neurons, whose apparent correlations (due to incomplete sampling) are reproduced with an intricate network of couplings J_{ij} [Cocco11c]. In practice, statistical error bars assess the relevance of inferred parameters, and overfitting is limited by penalties over large and/or small nonzero couplings.

Is the inverse problem well conditioned? Multi-electrode recordings give access to the activity of a limited part of the neural system under study. Would couplings change if more cells were to be recorded (Figure A)? The stability of the inferred couplings was tested in practice upon removal of one neuron from data. In DS1 the coupling between two RGC remained unchanged if their receptive field centers (RFC) are far from the RFC of the removed neuron [14]. In DS3 the identification of experience-related cell assemblies can be largely affected when the removed neuron is part of this assembly. The availability of massive optical recordings will soon allow for a better understanding of how well-conditioned are functional networks.

What happens if the model distribution is multimodal? The distribution of neural configurations S may be multimodal, and define largely different states of activity (B). If experimental data come from one state, can we trust the existence of other (not sampled) states predicted by the inferred model $P(S)$? A theoretical study of the Hopfield model, in which states are defined by the memorized items, gives a positive answer to this question, provided enough data are collected [27]; for limited sampling, an apparent connectivity matrix, specific to the state in which data are collected, will be inferred. Notice that extreme multimodality does not seem to be a generic feature of functional models inferred from neural data [14], contrary to “glassy” Ising models with random couplings (Figure B).



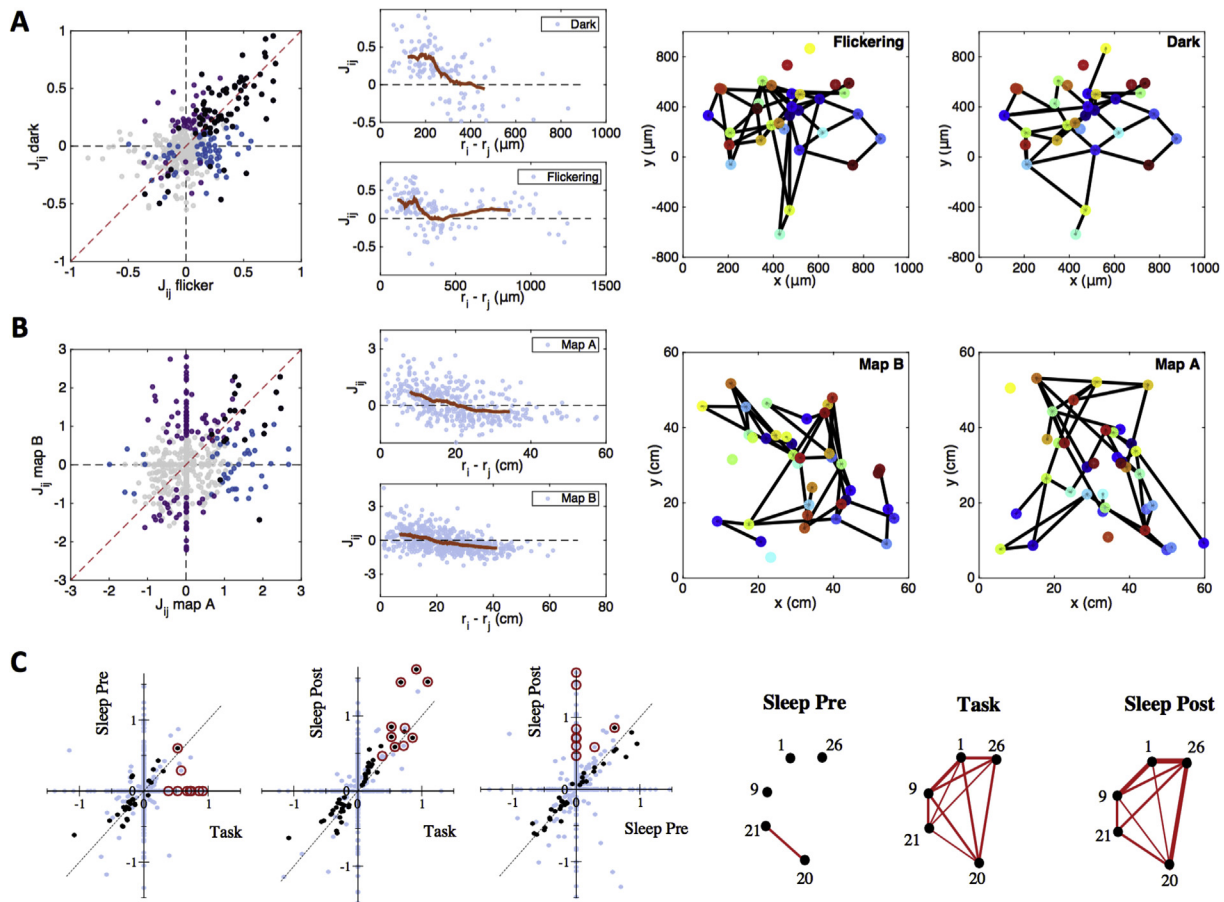
Sampling and inference. **A.** The recorded population of neurons is usually a small subset of the brain area under consideration. The inverse problem is well conditioned if the couplings J do not vary much when other neurons are recorded [59]. **B.** The distribution of neural configurations may have different modes, identifying specific activity states. The model distribution is inferred from one of these modes (purple or blue data). A glassy distribution would exhibit many low-lying states, see right edge of the panel.

and to the local pattern of bipolar and amacrine cells connecting photoreceptors to neighboring RGC. In addition, common inputs due to the visual stimulus in flicker conditions produce extra long-range effective couplings.

(DS2) the activities of CA1 hippocampal place cells were recorded, after a rat had been trained in two environments, identical in shape but differing by light

conditions [25]. Figure 1B shows that J_{ij} takes quite different values in the two associated cognitive maps for most pairs of cells i,j [17], emphasizing the functional differences between the inferred networks due to place field (PF) remapping [26]. These differences may be due to environment-specific cortical inputs to the hippocampus; they are also expected even if the hippocampal activity is generated by a *unique* physiological network, when limited sampling of the bimodal activity

Figure 1



Dependence of functional networks and couplings on external stimuli or conditions. **A.** Couplings were inferred from recordings of 32 retinal ganglion cells (RGC) in dark condition (Dark) and in presence of a flickering stimulus (Flicker) [14]. Data courtesy of M. Meister [4]. Left: Scatter plots of couplings J_{ij} in Flicker (x-axis) vs. J_{ij} in Dark (y-axis). Unreliable couplings, i.e. such that $|J_{ij}/\Delta J| < 3$, where ΔJ is the statistical error bar due to finite sampling, in both sessions are shown with grey dots. Black dots show reliable couplings in both sessions; couplings reliable in only one session are shown with purple (Dark) and blue (Flicker) dots. Middle: Couplings between pairs of neurons vs. distances between their receptive-field centers in Dark and Flicker conditions. Negative couplings are absent at short distances ($< 200 \mu\text{m}$) in Dark and Flicker conditions, and positive couplings are rare in Dark at large distances ($> 500 \mu\text{m}$), but not in Flicker. Red lines represent moving averages over 15 successive points. Right: Spatial maps of largest couplings ($J_{ij} > 0.3$). Links are connecting the receptive field centers (indicated by circles of different colors) of the recorded 32 cells in Dark and in Flicker. **B.** Couplings inferred from recordings of a population of 38 CA1 place cells as a rat explores two environments, A and B, differing by light conditions [17]. Data from Ref. [25]. Left: Scatter plots of couplings inferred from the reference session recordings of A (x-axis) vs. B (y-axis). Same color code as in panel A. Note the presence of many zero couplings, especially in the network associated to map A, due to the regularization in the inference procedure [55,42]. Middle: Couplings between pairs of neurons vs. distances between their place-field centers, estimated as the locations corresponding to maximal firing activities. Right: Spatial maps of the largest couplings ($J_{ij} > 0.5$) in the functional networks associated to maps A and B. Links are connecting the centers of the place fields, which are partially remapped across the two maps (each neuron is indicated by the same color in both maps). **C.** Couplings inferred from recordings of a population of 37 cells in the medial Prefrontal Cortex during the performance of a cross-modal task (Task), and in preceding (Sleep Pre) and following (Sleep Post) sleep periods [33,39]. Data from Ref. [7]. Left: Scatter plots of couplings in the three periods show the presence of conserved couplings, and a group of potentiated couplings supported by 5 cells (red circles). Reliable couplings in both periods are shown with dark dots. Right: subnetwork of couplings between those 5 cells in the three periods. Line thicknesses are proportional to intensities of couplings, all couplings shown are positive.

distribution is done around either of the memorized map [27] (Box 2).

The dependence of couplings upon distance between PF centers is similar in both maps (Figure 1B). The positivity of couplings at small distances (comparable to PF size), and negativity at larger distance, is compatible

with models of continuous attractors sustaining bump formation and motion [28–30].

(DS3) neurons in the prefrontal cortex of a behaving rat were recorded [7] during sessions, composed of a cross-modal rule shift task, preceded and followed by sleep periods, to study replay and memory consolidation

[5,31,32]. Figure 1C shows that most couplings are conserved across the sleep periods in a session, but a few undergo experience-related potentiation [33], which we study below.

Experience-related changes in functional connectivity and cell assemblies

The 'two-stage' theory of memory assumes that neural sequences formed during the awake period are transferred during sleep phases to cortical areas, such as medial prefrontal cortex, where they are memorized. This process of memory consolidation is concomitant to the onset of hippocampal excitations, called sharp-wave ripples [34], during which experience-related neural assemblies are replayed [5,7,23].

DS3 offers a natural test ground to study replay from the point of view of functional connectivity [18]. The neurons supporting the potentiated couplings in DS3 (Figure 1C) strongly coactivate during the task-performing and the subsequent sleep periods over few tens of ms [33], as expected for a cell assembly [35], but not in the preceding sleep epoch. It is possible that, in some sessions, the activation of the potentiated group mostly results from external inputs, in particular hippocampal ripples [34,7,36], and reflect early stages of learning; the corresponding functional networks are densely connected (Figure 1C), as expected when neurons are coactivated by a common input. In other sessions, the activation of the potentiated group does not seem to be related to ripples, and presumably corresponds to consolidated PFC networks, supporting memory-related cell assemblies [33].

Identifying a repeated replay-related cell assembly, with potential variations in the set of recruited neurons and in the relative timings of spikings, is a computationally hard task. The combinatorial nature of spatio-temporal possible sequences makes exhaustive search practically impossible unless templates, e.g. place-cell sequences in awake periods, are available [5,37,23,32]. Functional-connectivity-based approaches can help reveal cell assemblies without templates [38]. An approach based on direct simulations of the inferred model in the presence of an external drive, grossly mimicking hippocampal inputs, unveils groups of coactivating neurons, see Figure 2C [39].

Functional connectivity models reproduce multi-neuron statistics

Effective interactions are inferred from data to reproduce low-order statistics of firing events, such as the neuron firing rates and their pairwise correlations [12], see application to retina ganglion cell data in Box 1. Remarkably the model distribution (Box 1) is able to accurately predict higher order statistical features, such as the frequencies of coactivation of all triplets of

neurons, the probability that K out of the recorded cells are active in a time bin, and the frequencies of all 2^K possible patterns of activity of a subset of K cells [12,40] (Figure 2A). As a consequence, while functional pairwise models are trivially adequate for the modelling of very sparse activity data, e.g. in which two or less neurons are active in any time bin [41] (Box 2), their range of applicability extends in practice much beyond [42].

Specificity of functional model distributions allows for efficient state decoding

As seen above functional-connectivity-based models inferred in different conditions (states C) define accurate and condition-specific distributions $P^C(S)$ over neural population activities S (Box 1, Eq. [2]). Comparing and ranking different $P^C(S)$'s for a given S allows for decoding the unknown state, even in the absence of sensory correlate. Such an approach was applied in Ref. [17], to track the fast dynamics of retrieval of two cognitive maps (A & B) evoked by environmental light conditions subject to immediate switches, see DS2 above. Figure 2B represents the log-ratio $P^A(S_t)/P^B(S_t)$ of the activity configuration at time t , S_t . As found in the CA3 region of the hippocampus [25] we observe a short-term instability after the switch, extending over a few seconds, before stabilization of the internal map, coherently with the external light condition.

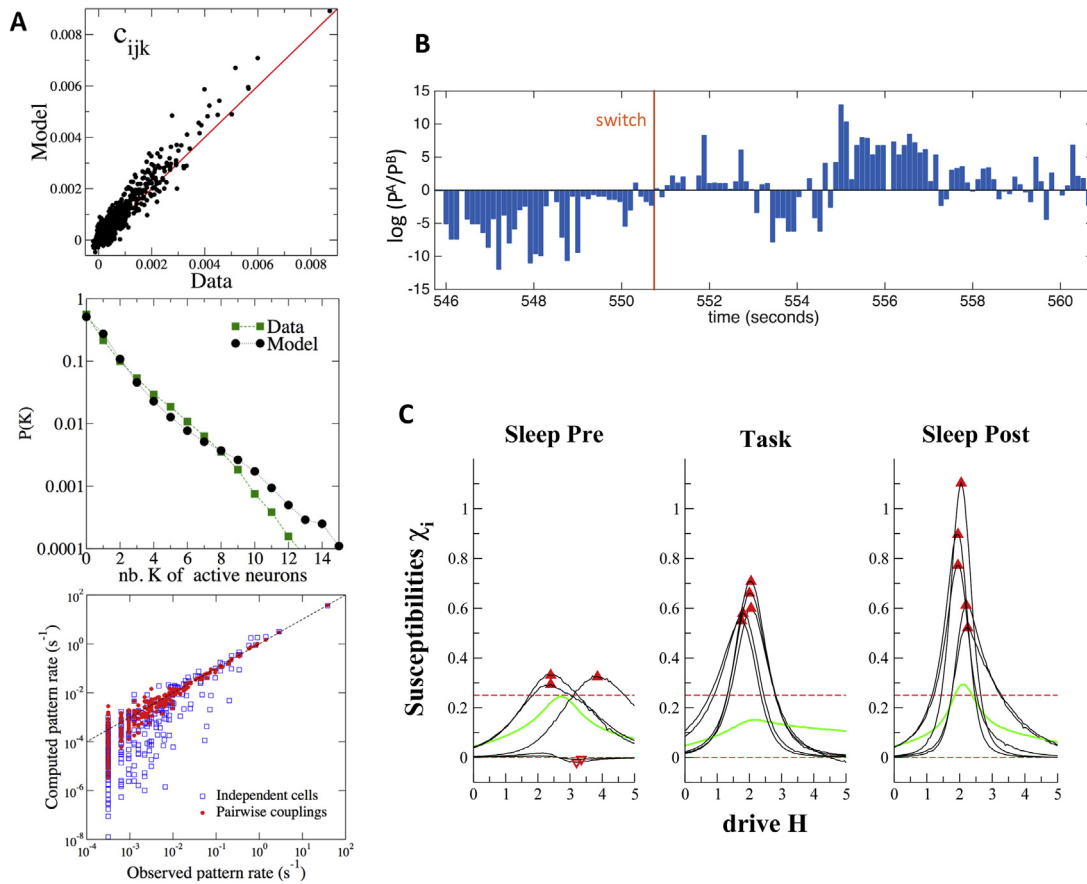
The decoding of maps is much harder in CA1 than in CA3, where remapping of PFs between environments is stronger and makes maps orthogonal. Yet functional-connectivity-based decoders show very good performances in CA1, and can detect map changes on very short time scales (few tens of ms), without any knowledge of the place fields and the animal position.

Similar information-theoretic approaches [16,43] were applied to decode visual stimuli from RGC activity, see for instance [40,44].

Extensions

Due to space limitations we have considered here models for activity snapshots only. As the precise ordering of spikes in a (narrow) time bin is not taken into account in the modeling the functional connectivity matrix is symmetric: the presence of a nonzero coupling J_{ij} signals a conditional dependence of the spiking events of neurons i and j , but is not informative about the causality between those events. Functional connectivity can also be inferred to capture some dynamical features in the neural data, e.g. with Generalized Linear Models (GLM) [45,46], Integrate-and-Fire Models (IF) [47,48], Kinetic Ising models [49,50]. Within these approaches couplings are not a priori symmetric, and could serve to define a temporal ordering in the sequence of activation events. However,

Figure 2



Predictive Power of Functional-Connectivity Models. **A.** Predictions for multi-neuron spiking frequencies from functional pairwise model. Top: Scatter plot of correlations $c_{ijk} = p_{ijk} - p_{ij}p_k - p_{ik}p_j - p_{jk}p_i + 2p_{ij}p_jp_k$ between triplets of cells; Middle: Probability of K neurons spiking in the same time window [42]; Bottom: Frequencies of all 2^{10} possible patterns of activity for a subpopulation of 10 neurons obtained from the independent (Blue) and the pairwise (Red) models are compared to the empirical frequencies in the data. Models were inferred after binning in $\Delta t = 20$ ms time windows of the activity of a population of $N = 40$ RGC. Data courtesy of M. Berry [12]. For the top and middle panels, predictions of model were obtained through Monte Carlo sampling [42]; for the bottom panel, predictions were obtained through an exact calculation. **B.** Decoding of hippocampal place-cell maps as function of time in a 'teleportation' experiment, in which maps are evoked by switches of light conditions [17]. Initially map B is retrieved, in agreement with the external light condition. Around $t \sim 551$ s (vertical red line) the light condition is abruptly switched to the one corresponding to environment A. The dynamically retrieved map is decoded from the activity configuration at time t , S_t , based on the sign of the log. ratio of $P^A(S_t)/P^B(S_t)$ (y-axis), where P^A , P^B are the model distributions inferred in both environment in stable conditions (no switch, reference sessions) [17]. An instability period is observed for few seconds after the light switch. Data from K. Jezek (N = 38 CA1 place cells) [25]. **C.** Identification of replay-related cell assemblies in medial Prefrontal Cortex [39]. Data from F. Battaglia (37 recorded cells) [7]. After inference of the functional model from spiking activity in each one of the three periods (see text and caption Figure 1C) the model is simulated under the action of an external input (drive H), added to the argument of Φ , Eq. [1] of Box 1 [39]. Plots show the susceptibility, that is, the derivative of the average value of s_i with respect to H, for the 5 cells i identified in the subnetwork of Figure 1C. The green curve is the average susceptibility χ over the remaining 32 cells; the dotted line $\chi = \frac{1}{4}$ corresponds to the top susceptibility for an independent cell. In the Task and Sleep Post periods the same cell assembly is found, corresponding to a group of 5 cells, whose activities maximally respond to the same value of the drive (top susceptibilities, red triangles) In the Sleep Pre period this assembly does not exist: the top three susceptibilities barely exceed what is expected for independent neurons, and the remaining two cells do not respond at all to comparable drive.

couplings are often close to being symmetric [14,39], especially if the bin width used for their inference is comparable to (or larger than) synaptic delays [48]. Note that those models are not generative, as they make extra assumptions with respect to maximum entropy models, e.g. GLM often assumes that the neural spiking activity is Poissonian. Moreover it is crucial to reduce the number of free parameters to avoid overfitting data.

To end with, while this review has focused on functional models with pairwise couplings only, different approaches have been introduced to infer multi-neuron interaction at higher orders [14,51–53]. The existence of multi-neuron connectivity is expected due to the presence of common inputs coming from nonrecorded cells. Restricted Boltzmann machines [54], in which effective, high-order couplings are introduced through additional hidden variables, were recently applied to cortical microcolumn data. How

important these effective multi-neuron interactions are remains an open question.

Acknowledgments

This article is based on collaborations with JP Barton, FP Battaglia, K Jezek, S Leibler, U Ferrari, S Rosay. We are grateful to L Bourdieu, G Debregeas, JF Leger, C Ventalon for useful discussions. This work was partly funded by the [EU-] FP7 FET OPEN Enlightenment 284801 and the HFSP RGP0057/2016 projects.

References

Papers of particular interest, published within the period of review, have been highlighted as:

- * of special interest
- ** of outstanding interest

1. Gerstein GL, Perkel DH: **Simultaneously recorded trains of action potentials: analysis and functional interpretation.** *Science* 1969, **164**(3881):828–830.
2. Aersten AM, Gerstein GL, Habib MK, Palm G: **Dynamics of neuronal firing correlations: modulation of 'effective connectivity'.** *J Neurophysiol* 1989, **61**(5):900–917.
3. McNaughton BL, O'Keefe J, Barnes CA: **The stereotrode: a new technique for simultaneous isolation of several single units in the central nervous system from multiple unit records.** *J Neurosci Methods* 1983, **8**(4):391–397.
4. Meister M, Pine J, Baylor DA: **Multi-neuronal signals from the retina: acquisition and analysis.** *J Neurosci Methods* 1994, **51**(1):95–106.
5. Wilson MA, McNaughton BL: **Reactivation of hippocampal ensemble memories during sleep.** *Science* 1994, **265**(5172):676–679.
6. Nicolelis MA: *Methods for neural ensemble recordings.* CRC press; 2007.
7. Peyrache A, Khamassi M, Benchenane K, Wiener SI, Battaglia FP: **Replay of rule-learning related neural patterns in the prefrontal cortex during sleep.** *Nat Neurosci* 2009, **12**(7):919–926.
- Estimation of replay and related cell assemblies, based on extraction of 'templates' through principal component analysis.
8. Bathellier B, Ushakova L, Rumpel S: **Discrete neocortical dynamics predict behavioral categorization of sounds.** *Neuron* 2012, **76**(2):435–449.
9. Wolf S, Supatto W, Debregeas G, Mahou P, Kruglik SG, Sintès JM, Beaupaire E, Candelier R: **Whole-brain functional imaging with two-photon light-sheet microscopy.** *Nat Methods* 2015, **12**(5):379–380.
10. Friston KJ: **Functional and effective connectivity: a review.** *Brain Connect* 2011, **1**(1):13–36.
- General introduction to functional connectivity, with special emphasis on applications to fMRI data.
11. Stevenson IH, Rebesch JM, Miller LE, Koerting KP: **Inferring functional connections between neurons.** *Curr Opin Neurobiol* 2008, **18**(6):582–588.
12. Schneidman E, Berry MJ, Segev R, Bialek W: **Weak pairwise correlations imply strongly correlated network states in a neural population.** *Nature* 2006, **440**(7087):1007–1012.
- Analysis of retinal activity snapshots with probabilistic graphical models. At the basis of many of the articles reviewed here.
13. Shlens J, Field GD, Gauthier JL, Grivich MI, Petrusca D, Sher A, Litke AM, Chichilnisky EJ: **The structure of multi-neuron firing patterns in primate retina.** *J Neurosci* 2006, **26**(32):8254–8266.
14. Cocco S, Leibler S, Monasson R: **Neuronal couplings between retinal ganglion cells inferred by efficient inverse statistical physics methods.** *Proc Natl Acad Sci USA* 2009, **106**(3):14058–14062.
15. Brown EN, Frank LM, Tang D, Quirk MC, Wilson MA: **A statistical paradigm for neural spike train decoding applied to position prediction from ensemble firing patterns of rat hippocampal place cells.** *J Neurosci* 1998, **18**(18):7411–7425.
16. Quiroga RQ, Panzeri S: **Extracting information from neuronal populations: information theory and decoding approaches.** *Nat Rev Neurosci* 2009, **10**(3):173–185.
17. Posani L, Cocco S, Jezek K, Monasson R: **Functional connectivity models for decoding of spatial representations from hippocampal CA1 recordings.** *J Comput Neurosci* 2017. **10**:1007s10827-017-0645-9.
18. Holtmaat A, Caroni P: **Functional and structural underpinnings of neuronal assembly formation in learning.** *Nat Neurosci* 2016, **19**(12):1553–1562.
- A review of recent experimental progresses in studying cell assemblies and memory consolidation.
19. Carrillo-Reid L, Yang W, Bando Y, Peterka DS, Yuste R: **Imprinting and recalling cortical ensembles.** *Science* 2016, **353**(6300):691–694.
20. Hopfield JJ: **Neural networks and physical systems with emergent collective computational abilities.** *Proc Nat Acad Sci* 1982, **79**(8):2554–2558.
21. Bliss TV, Collingridge GL: **A synaptic model of memory: long-term potentiation in the hippocampus.** *Nature* 1993, **361**(6407):31–39.
22. Harris KD, Csicsvari J, Hirase H, Dragoi G, Buzsáki G: **Organization of cell assemblies in the hippocampus.** *Nature* 2003, **424**(6948):552–556.
- One of the first works on the identification of cell assemblies from hippocampal data.
23. O'Neill J, Pleydell-Bouverie B, Dupret D, Csicsvari J: **Play it again: reactivation of waking experience and memory.** *Trends Neurosci* 2010, **33**(5):220–229.
24. Wilber A, Skelin I, McNaughton BL: **Laminar organization of encoding and memory reactivation in the parietal cortex.** *bioRxiv* 2017, <http://dx.doi.org/10.1101/110684>.
25. Jezek K, Henriksen EJ, Treves A, Moser EI, Moser M: **Theta-paced flickering between place-cell maps in the hippocampus.** *Nature* 2011, **478**(7368):246–249.
26. Muller RU, Kubie JL: **The effects of changes in the environment on the spatial firing of hippocampal complex-spike cells.** *J Neurosci* 1987, **7**(7):1951–1968.
27. Cocco S, Monasson R, Sessak V: **High-Dimensional inference with generalized Hopfield model : principal component analysis and corrections.** *Phys Rev E* 2011, **83**(5):051123.
28. Tsodyks M, Sejnowski T: **Associative memory and hippocampal place cells.** *Int J Neural Syst* 1995, **6**:81–86.
29. Battaglia FP, Treves A: **Attractor neural networks storing multiple space representations: a model for hippocampal place fields.** *Phys Rev E* 1998, **58**(6):7738.
30. Monasson R, Rosay S: **Transitions between spatial attractors in place-cell models.** *Phys Rev Lett* 2015, **115**(9):098101.
31. Lee AK, Wilson MA: **Memory of sequential experience in the hippocampus during slow wave sleep.** *Neuron* 2002, **36**(6):1183–1194.
32. Carr MF, Jadhav SP, Frank LM: **Hippocampal replay in the awake state: a potential substrate for memory consolidation and retrieval.** *Nat Neurosci* 2011, **14**(2):147–153.
33. Tavoni G, Ferrari U, Battaglia FP, Cocco S, Monasson R: **Inferred model of the prefrontal cortex activity unveils cell assemblies and memory replay.** *Netw Neurosci* 2017. http://dx.doi.org/10.1162/NETN_a_00014.
34. Buzsáki G: **Hippocampal sharp wave-ripple: a cognitive biomarker for episodic memory and planning.** *Hippocampus* 2015, **25**(10):1073–1188.
35. Buzsáki G: **Neural syntax: cell assemblies, synapsemes, and readers.** *Neuron* 2010, **68**(3):362–385.

36. Girardeau G, Benchenane K, Wiener SI, Buzsáki G, Zugaro MB: **Selective suppression of hippocampal ripples impairs spatial memory.** *Nat Neurosci* 2009, **12**(10):1222–1223.
37. Fujisawa S, Amarasingham A, Harrison MT, Buzsáki G: **Behavior-dependent short-term assembly dynamics in the medial prefrontal cortex.** *Nat Neurosci* 2008, **11**(7):823–833.
38. Billeh YN, Schaub MT, Anastassiou CA, Baharona M, Koch C: **Revealing cell assemblies at multiple levels of granularity.** *J Neurosci Methods* 2014, **236**:92–106.
39. Tavoni G, Cocco S, Monasson R: **Neural assemblies revealed by inferred connectivity-based models of prefrontal cortex recordings.** *J Comp Neurosci* 2016, **41**(3):269–293.
40. Granot-Atedgi E, Tkačik G, Segev R, Schneidman E: **Stimulus-dependent maximum entropy models of neural population codes.** *PLoS Comput Biol* 2013, **9**(3):e1002922.
41. Roudi Y, Nirenberg S, Latham PE: **Pairwise maximum entropy models for studying large biological systems: when they can work and when they can't.** *PLoS Comput Biol* 2009, **5**(5):e1000380.
42. Barton J, Cocco S: **Ising models for neural activity inferred via selective cluster expansion: structural and coding properties.** *J Stat Mech* 2013, **2013**(03):P03002.
43. Tkačik G, Prentice JS, Balasubramanian V, Schneidman E: **Optimal population coding by noisy spiking neurons.** *Proc Natl Acad Sci USA* 2010, **107**(32):14419–14424.
44. Marre O, Botella-Soler V, Simmons KD, Mora T, Tkačik G, Berry MJ: **High accuracy decoding of dynamical motion from a large retinal population.** *PLoS Comput Biol* 2015, **11**(7):e1004304.
45. Truccolo W, Eden UT, Fellows MR, Donoghue JP, Brown EN: **A point process framework for relating neural spiking activity to spiking history, neural ensemble, and extrinsic covariate effects.** *J Neurophysiol* 2005, **93**(2):1074–1089.
- One of the first applications of GLM to neural data.
46. Pillow JW, Shlens J, Paninski L, Sher A, Litke AM, Chichilnisky EJ, Simoncelli EP: **Spatio-temporal correlations and visual signalling in a complete neuronal population.** *Nature* 2008, **454**(7207):995–999.
47. Koyama S, Paninski L: **Efficient computation of the maximum a posteriori path and parameter estimation in integrate-and-fire and more general state-space models.** *J Comput Neurosci* 2010, **29**(1–2):89–105.
48. Monasson R, Cocco S: **Fast inference of interactions in assemblies of stochastic integrate-and-fire neurons from spike recordings.** *J Comput Neurosci* 2011, **31**(2):199–227.
49. Marre O, El Boustani S, Fregnac Y: **Destexhe A: prediction of spatiotemporal patterns of neural activity from pairwise correlations.** *Phys Rev Lett* 2009, **102**(13):138101.
50. Dunn B, Morreaunet M, Roudi Y, Correlations, Functional: **Connections in a population of grid cells.** *PLoS Comput Biol* 2015, **11**(2):e1004052.
51. Ganmor E, Segev R, Schneidman E: **Sparse low-order interaction network underlies a highly correlated and learnable neural population code.** *Proc Natl Acad Sci U S A* 2011, **108**(23):9679–9684.
52. Gardella C, Marre O, Mora T: **A tractable method for describing complex couplings between neurons and population rate.** *Eneuro* 2016, **3**(4):0160–15.
53. O'Donnell C, Goncalves JT, Whiteley N, Portera-Cailliau C, Sejnowski TJ: **The population tracking model: a simple, scalable statistical model for neural population data.** *Neural Comput* 2017, **29**(50):93.
54. Köster U, Sohl-Dickstein J, Gray CM, Olshausen BA: **Modeling higher-order correlations within cortical microcolumns.** *PLoS Comput Biol* 2014, **10**(7):e1003684.
- Derivation of high-order effective connectivity with restricted Boltzmann machines, which goes beyond usual pairwise functional models.
55. Cocco S, Monasson R: **Adaptive cluster expansion for inferring Boltzmann machines with noisy data.** *Phys Rev Lett* 2011, **106**(9):090601.
56. Hinton GE, Sejnowski TJ: **Learning and relearning in Boltzmann machines.** In *Explorations in the microstructure of cognition 1: foundations*. Edited by McClelland J, Rumelhart D, Cambridge: MIT Press; 1986:282–317.
57. Broderick T, Dudik M, Tkačik G, Schapire RE, Bialek W: **Faster solutions of the inverse pairwise Ising problem.** arXiv Preprint. 2007 arXiv:0712.2437.
58. Ravikumar P, Wainwright MJ, Lafferty JD: **High-dimensional Ising model selection using L₁-regularized logistic regression.** *Ann Statistics* 2010, **38**(3):1287–1319.
59. Cocco S, Monasson R: **Adaptive cluster expansion for the inverse Ising problem: convergence, algorithm and tests.** *J Stat Phys* 2012, **147**(2):252–314.